Transport properties of composition tuned α- and β-$Eu_8Ga_{16-x}Ge_{30+x}$

A. Bentien, V. Pacheco,* S. Paschen,† Yu. Grin, and F. Steglich
Max Planck Institute for Chemical Physics of Solids, Nöthnitzer Str. 40, D-01187 Dresden, Germany
(Received 11 March 2004; revised manuscript received 15 October 2004; published 18 April 2005)

This paper presents the transport properties of several composition tuned α- and β-$Eu_8Ga_{16-x}Ge_{30+x}$ samples where $0.28 \leqslant x \leqslant 0.48$ for the α samples and $0.49 \leqslant x \leqslant 1.01$ for the β samples. Among samples with the same structure (α or β), the varying physical properties can be understood in terms of a rigid conduction band where only the charge carrier concentration is varied. The differences in the physical properties between α and β samples can be explained by a charge-carrier effective mass (m^*) that is more than three times larger in the β phase than in the α phase. As a result of the low charge-carrier mobility we argue that the thermoelectric figure of merit of *n*-type α- and β-$Eu_8Ga_{16-x}Ge_{30+x}$, without modifications to enhance the thermoelectric properties, will not exceed that of the best materials at room temperature. From modeling the lattice thermal conductivity (κ_L) of α- and β-$Eu_8Ga_{16-x}Ge_{30+x}$, it is proposed that κ_L of all clathrates with divalent cations can be described by phonon-charge-carrier scattering at low temperatures and resonant scattering at higher temperatures. This contradicts earlier models where the low-temperature κ_L of β-$Eu_8Ga_{16}Ge_{30}$ and $Sr_8Ga_{16}Ge_{30}$ is modeled by scattering of phonons from tunneling states. However, since the phonon-charge-carrier scattering rate increases with $(m^*)^2$ the advantage of the phonon-charge-carrier scattering model is the ability to explain the lower low-temperature κ_L of β-$Eu_8Ga_{16-x}Ge_{30+x}$, compared to α-$Eu_8Ga_{16-x}Ge_{30+x}$.

DOI: 10.1103/PhysRevB.71.165206 PACS number(s): 72.20.Pa, 75.50.Cc, 72.15.Jf

I. INTRODUCTION

Within the last several years research in thermoelectric materials has gained interest due to the discovery of sets of materials that show promising thermoelectric properties, e.g., $CsBi_4Te_6$,[1] Tl_9BiTe_6,[2] Zn_4Sb_3,[3] and clathrates.[4] Usually, thermoelectric properties are benchmarked by the dimensionless thermoelectric figure of merit $ZT = S^2T\sigma/\kappa$, where S is the thermopower, σ the electrical conductivity, κ the thermal conductivity, and T the temperature. Of the above-mentioned materials only Zn_4Sb_3 has a ZT above 1, but at elevated temperatures; and for the past four decades, the state-of-the-art materials are alloys based on Bi_2Te_3 with $ZT \sim 1$ at room temperature. However, new strategies in the search for enhanced thermoelectric materials makes a ZT beyond 2 at room temperature not an unrealistic goal. Our approach is to search for so-called Kondo insulators[5] in systems with low thermal conductivity. Kondo insulators are known to have an enhanced electronic density of states around the Fermi level, which enhances the power factor ($S^2\sigma$). Until now are α- and β-$Eu_8Ga_{16-x}Ge_{30+x}$ the only two clathrates where the cages are completely filled with rare-earth elements; it is our hope that by either modifying these two materials or introduction of different rare-earth elements a Kondo insulating clathrate can be obtained.

Inorganic clathrates with divalent cations were discovered in the mid-1980s.[6] Their physical properties remained unknown until Nolas *et al.* measured σ, S, and κ of three samples of $Sr_8Ga_{16}Ge_{30}$ with relatively good thermoelectric properties.[4] Since then an increasing number of papers treating the physical and transport properties have been published.[7–10] Band structure calculations predict all clathrates with divalent cations and the ideal stoichiometry 8:16:30 to be semiconductors with band gaps ε_g ranging from approximately 0.3 to 0.9 eV depending on composition and calculation method.[11–13] Until now most clathrate samples show metal-like properties but with a low concentration of carriers (n). Only for a few samples semiconducting properties have been observed;[4,7,10,14] the carriers appear to be excited from impurity-like levels. Bryan *et al.* explain the metallic properties of $Ba_8Ga_{16}Ge_{30}$ with small deviations from the ideal Ga/Ge ratio, although vacancies could not be excluded.[9] Anno *et al.* were able to synthesize both *p*- and *n*-type $Ba_8Ga_{16}Ge_{30}$ by varying the Ga/Ge starting composition.

This paper is the second of two back-to-back papers. In the first one[15] we have shown that it is possible to control n within the homogeneity range by the preparation route and that there is a close relationship between the composition of α- and β-$Eu_8Ga_{16-x}Ge_{30+x}$ and n. This can be represented by the formula $Eu_8Ga_{16-x}Ge_{30+x}$, where $n \sim x$ (if n is in units of carriers per unit cell, e^-/u.c.) for the samples used in the present paper. We have earlier reported on the structural and physical properties of α- and β-$Eu_8Ga_{16}Ge_{30}$.[8] The α phase corresponds to the clathrate-VIII-type structure in which also $Ba_8Ga_{16}Sn_{30}$ crystallizes,[6] whereas the β phase has clathrate-I-type structure. Both materials order ferromagnetically at approximately 10.5 K and 36 K for the α and β phase, respectively.[8] Seven α phase samples and four β phase samples with varying n have been prepared. They are hereafter referred to as $\alpha 1, 2, \ldots, 7$ and $\beta 1, 2 \ldots, 4$. Some initial results on the β samples have been published in Ref. 16. The two samples from our earlier publication[8] are also included as $\alpha 8$ and $\beta 5$.

In Sec. II we present the transport properties of all samples. In Sec. III we analyze the charge-carrier transport properties for samples of the same phase and show that the variation can be understood in terms of a rigid parabolic band model where only n is varied because of a variation in the Ga-Ge composition. In Sec. IV we analyze the phonon

TABLE I. Selected measured and calculated parameters for α- and β-$Eu_8Ga_{16-x}Ge_{30+x}$. For the calculated parameters a free-electron model has been assumed. The charge carrier concentration (n) is calculated from the Hall resistivity as function of magnetic field at 2 K by assuming a one band model with a Hall scattering factor of unity. Data have been corrected for anomalous Hall scattering.[15] The charge carrier effective mass (m_B^*) is calculated from the thermopower at 400 K and n assuming that phonon scattering dominates. However, this seems to overestimate m_B^* for the α-$Eu_8Ga_{16}Ge_{30}$ samples (see text). The mean-free path of the charge carriers at 2 K [l_e(2 K)] is calculated from the electrical resistivity at 2 K [ρ(2 K)] and n. The Fermi temperature (T_F) is calculated from the thermopower at 400 K. RRR is the residual resistance ratio [ρ(400 K)/ρ(2 K)]. x is the off-stoichiometry ($Eu_8Ga_{16-x}Ge_{30+x}$) given in Ref. 15. Samples are sorted according to increasing n. See text for further explanation.

Sample	n(2 K) (e^-/u.c.)	ρ(2 K) (mΩ cm)	m_B^* (m_0)	l_e(2 K) (Å)	T_F (K)	RRR	x
α4	0.143	2.425	1.50	21.7	681	1.24	0.42
α6	0.160	1.705	1.48	28.6	746	1.44	0.28
α2	0.170	1.878	1.59	24.9	723	1.20	0.34
α1	0.176	1.417	1.60	32.3	735	1.41	0.34
α5	0.194	1.043	1.59	41.0	791	1.57	0.44
α7	0.231	0.502	1.44	75.9	981	1.99	0.42
α3	0.267	0.902	1.86	38.4	834	1.51	0.36
α8	0.461	0.290	1.46	82.9	1531	3.00	0.48
β1	0.431	0.894	3.10	28.6	679	2.28	0.53
β3	0.633	0.662	3.09	29.9	880	2.38	0.48
β2	0.939	0.565	3.85	26.9	919	2.23	0.47
β4	0.986	0.544	3.00	27.0	1219	2.24	0.76
β5	1.529	0.299	3.25	36.8	1507	2.47	1.01

transport properties and challenge the literature models where the low-temperature lattice thermal conductivity (κ_L) is modeled by phonon scattering on tunneling states. Instead we propose that phonon scattering on charge carriers has to be considered and that the large difference in κ_L between α- and β-$Eu_8Ga_{16}Ge_{30}$ is closely related to the electronic band structure of the two compounds.

In the following the abbreviation $(Ba/Sr/Eu)_8Ga_{16}Ge_{30}$ will be used for $Ba_8Ga_{16}Ge_{30}$, $Sr_8Ga_{16}Ge_{30}$, and $Eu_8Ga_{16}Ge_{30}$.

II. PHYSICAL PROPERTIES

On all samples the electrical resistivity ρ has been measured as function of temperature with a standard four-point ac method. Hall resistivity ρ_H measured as function of magnetic field (B) at 2 K has been used to determine n.[15] κ and S as function of temperature were measured with the thermal transport option (TTO) from Quantum Design using a four-point method. It is based on a quasistatic technique described in Ref. 17. Low-temperature specific heat C_p was measured in a ^{3}He cryostat using a relaxation time method.

Table I summarizes selected physical properties of the samples that will be discussed later in the text. In Fig. 1, $\rho(T)$ is shown for the α and β samples. ρ increases with increasing temperature except for a narrow range above the magnetic ordering temperature T_c where the $\partial\rho/\partial T$ is negative. For all samples $\rho(T)=\rho_0+AT^2$ at lowest temperatures. This type of temperature dependence is expected for scattering of electrons on spinwaves.[18] A increases for samples with increasing ρ. Above approximately 100 K, $\rho(T)$ is linear for all samples. For the α samples the scattering from critical magnetic fluctuations, believed to be responsible for the anomaly in $\rho(T)$,[8] increases for samples with increasing ρ. The relative height of the anomaly, taken as the local maximum divided by the local minimum of ρ, increases from 1.05 for sample α8 to 1.37 for sample α4. From the inset of Fig. 1(a) it can be seen that the residual resistance ratio (RRR) decreases with increasing ρ(2 K). The magnitude of ρ among the α samples differs significantly, e.g., is ρ(2 K) $=0.29$ mΩ cm for sample α8 and ρ(2 K)$=2.4$ mΩ cm for sample α4. Within experimental resolution the effect of scattering from critical magnetic fluctuations does not vary among the β samples. As can be seen from the inset of Fig. 1(b) this is also the case for the RRR, which changes less than 5% among all β samples. $\rho(T)$ for the β samples is generally lower than for the α samples: ρ(2 K) $=0.30$ mΩ cm for sample β5 and 0.90 mΩ cm for sample β1.

Figure 2 shows $S(T)$ for the α and β samples. For both phases S has similar magnitude, but there is a strong composition dependence. S(300 K) decreases from -74 to -132 μV/K for sample $\alpha8-\alpha4$, and from -60 to -130 μV/K, for sample $\beta5-\beta1$. All samples show an almost linear temperature dependence above $\sim$50 K as expected if n is temperature independent.

The measurements of $\rho(T)$ and $S(T)$ on a single crystalline β-$Eu_8Ga_{16}Ge_{30}$ sample in Ref. 20 is in good agreement with

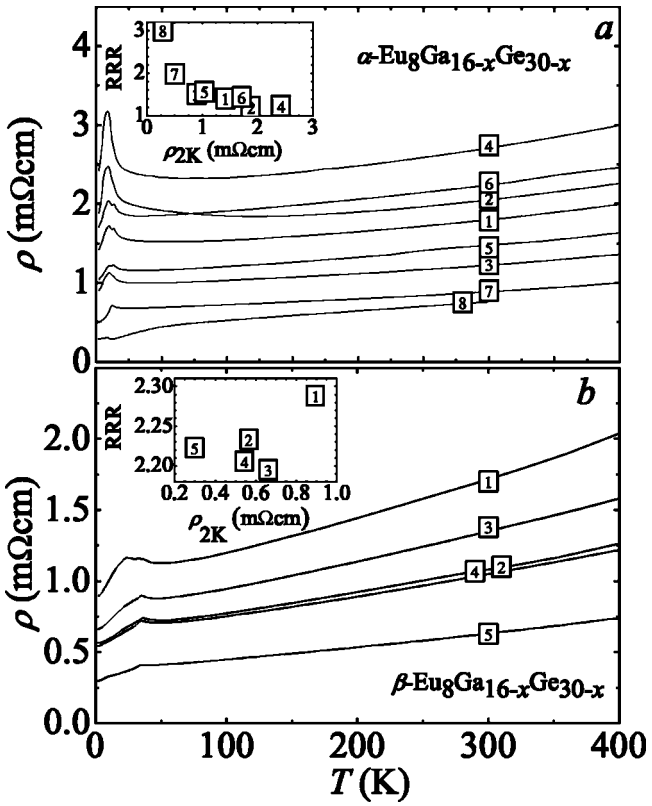

FIG. 1. Electrical resistivity (ρ) as function of temperature (T) for the α-$Eu_8Ga_{16-x}Ge_{30+x}$ samples (a) and the β-$Eu_8Ga_{16-x}Ge_{30+x}$ samples (b). Insets show the residual resistance ratio [RRR $=\rho(400\ \mathrm{K})/\rho(2\ \mathrm{K})$] as function of $\rho(2\ \mathrm{K})$.

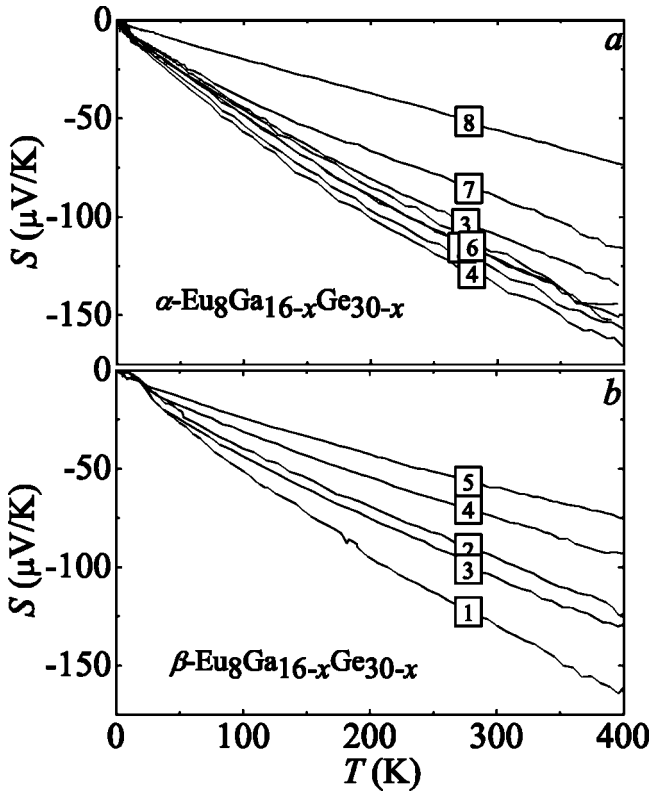

FIG. 2. Thermopower (S) as function of temperature (T) for the α-$Eu_8Ga_{16-x}Ge_{30+x}$ samples (a) and the β-$Eu_8Ga_{16-x}Ge_{30+x}$ samples (b).

our results. $\rho(T)$ of the sample is about 75% of that of $\beta 5$, the temperature dependence and the RRR is the same. $S(T)$ of the sample is slightly lower than that of $\beta 5$. In combination with our data it appears as if the charge carrier concentration is slightly larger than 1.5 electrons per unit cell in reasonable agreement with the estimate of Ref. 19.

Figure 3 shows the lattice thermal conductivity (κ_L) as function of temperature for the α and β samples. $\kappa_L(T)$ was calculated by subtracting the electronic contribution (κ_e), calculated from $\rho(T)$ using the Wiedemann-Franz law, from $\kappa(T)$. $\kappa_e(200\ \mathrm{K})$ ranges between 0.2 and 0.8 W/(Km) and decreases almost linearly with decreasing temperature. Below approximately 100 and 20 K the contribution from κ_e to κ starts to be negligible for the α and β samples, respectively. At low temperatures $\kappa_L(T) \propto T^{1.1-1.5}$ for the α samples, which is followed by a maximum at $\sim$6.5 K. Above 10 K, $\kappa_L(T)$ decreases with T^{-1} up to approximately 25 K whereupon κ_L decreases monotonically with temperature. The inset of Fig. 3(a) shows that $\kappa_L(193\ \mathrm{K})$, for the α phase, increases with both RRR and n. $\kappa_L(T)$ of the β samples resembles previously published data.[19,20] A broad dip in κ_L, observed at approximately 10 K, is believed to be due to resonant scattering of the phonons from the cations.[8,19,20] The inset of Fig. 3(b) shows $\kappa_L(193\ \mathrm{K})$ as function of RRR and n for the β samples, and it is seen that a correlation between $\kappa_L(193\ \mathrm{K})$ and RRR or n is not as clear as for the α samples.

III. CHARGE CARRIER TRANSPORT

Band structure calculations performed on the clathrate I and VIII structure type all come to the result that $(Sr/Ba/Eu)_8Ga_{16}Ge_{30}$ are semiconductors.[11–13] ε_g calculated for $Eu_8Ga_{16}Ge_{30}$ in the ferromagnetically ordered state is 0.37 and 0.48 eV for the α and β phase, respectively.[13] Because of spin splitting of the valence and conduction band ε_g is expected to be larger above T_c. However such calculations do not account for the effect of vacancies, which results in states in the forbidden gap.[21,22] The effect of the random positioning of Ga/Ge is difficult to predict, but it may be assumed that the band edges close to the forbidden gap are smeared out, giving rise to impurity-like states. It is generally assumed that a deviation from the ideal stoichiometry in both type I and VIII $(Sr/Ba/Eu)_8Ga_{16-x}Ge_{30+x}$ leads to n-type properties for $x>0$ because Ge excess adds electrons to the rigid conduction band and to p-type properties for $x<0$ because Ga excess adds holes to the rigid valence band. To justify this assumption we note that the Hall coefficient of $(Ba/Sr)_8Ga_{16}Ge_{30}$ samples (not shown), with n similar to the samples presented in this paper, has a very small temperature dependence. As was shown in our companion paper,[15] the temperature dependence of the Hall effect for α- and β-$Eu_8Ga_{16-x}Ge_{30+x}$ can be explained by the temperature dependence of the anomalous Hall effect. This indicates that the Fermi level (ε_F) is located well above the conduction band edge, and the disorder and/or vacancy states in the forbidden gap do not influence the transport properties unless

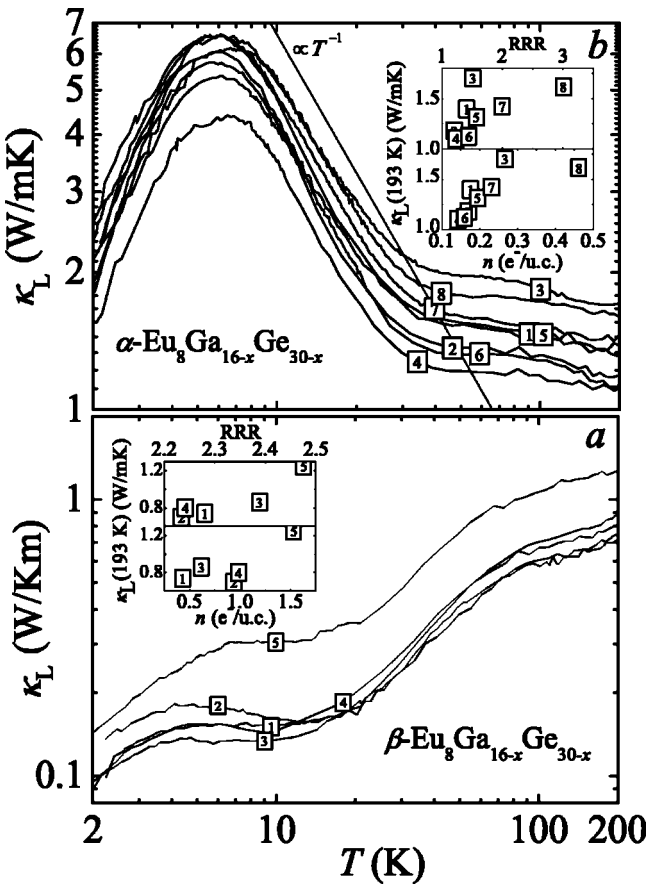

FIG. 3. Lattice thermal conductivity (κ_L) as function of temperature (T) for the α-$Eu_8Ga_{16-x}Ge_{30+x}$ samples (a) and the β-$Eu_8Ga_{16-x}Ge_{30+x}$ samples (b). The electronic part has been subtracted using the Wiedemann-Franz law. Insets show κ_L(193 K) as function of the residual resistance ratio [RRR=ρ(400 K)/ρ(2 K)] and carrier concentration at 2 K (n).

$k_BT > \varepsilon_F$. When ε_F is below the conduction band edge this may no longer be the case and semiconducting samples do, in fact, show a small activation energy,[4,7,14] which can be associated with the excitation of carriers from impurity-like states to the conduction or valence band.

Table I compares measured and calculated free electron model properties where the electron energy is taken to be zero at the conduction band minimum. All parameters that include n have been calculated assuming a Hall-scattering factor (A) of unity. However, band structure calculations give $A=0.59$ and 0.65 for charge carriers in the conduction band for α- and β-$Eu_8Ga_{16-x}Ge_{30+x}$, respectively.[13] This leads to slightly smaller values for n and the effective mass m^* and to a larger electron mean-free path l_e, but leaves the Fermi temperature T_F unchanged. If the calculated ε_g are assumed to be correct, then a simple calculation shows that the number of intrinsic carriers excited from the valence into the conduction band at temperatures up to 400 K is negligible compared to the extrinsic carriers that come from small deviations in the stoichiometry. T_F is larger than ~700 K for all samples; thus ε_F exceeds k_BT and the Sommerfeld expansion is valid. The clathrate materials investigated in the present paper can therefore be regarded as metals with a low concentration of degenerate carriers. This is also supported by the fact that $\rho(T)$ and $S(T)$ are linear in temperature above ~100 K, which is not likely to occur if either n changes with temperature or $T > T_F$. In the following we analyze the measured physical properties and show that the different properties among the α and β samples can be understood in terms of a parabolic rigid free-electron band where only n is changed.

The electrical conductivity σ in metals can be described by the general result derived from the semiclassical transport theory [see, e.g., Ref. 23 for further details of Eqs. (1)–(5)]

$$\sigma = \frac{e\tau}{m^*}\frac{1}{R_H}. \tag{1}$$

τ is the charge carrier relaxation time and e is the electron charge. For charge carriers scattered by acoustic phonons $\tau = \tau_0\varepsilon^{-1/2}$, where ε is the electron energy and τ_0 is a constant. In the free-electron model the speed of the electrons at the Fermi surface is $v_F \propto \varepsilon_F^{1/2}$ and l_e becomes independent of ε_F, leading to the explicit n dependence

$$\sigma = \frac{e^2 l_e}{3\pi^2\hbar}(3\pi^2 n)^{2/3}. \tag{2}$$

If electrons are scattered from impurities, then the relaxation time has the energy dependence $\tau = \tau_0\varepsilon^{3/2}$, leading to

$$\sigma = \frac{3\pi^2 e^2\hbar^3\tau_0}{2^{3/2}m^{*5/2}}n^2. \tag{3}$$

The dependence of σ on n due to scattering from the magnetic moments does not follow any simple power law. However, at $T \gg T_c$, $\sigma \propto n^{2/3}/m^{*2}$,[24] the same dependence as for scattering from acoustic phonons. Below T_c there is no general relationship, however, as T approaches zero so does the scattering rate. As can be seen from Fig. 1 the effect of the magnetic moments on $\rho(T)$ is only significant at temperatures around the magnetic ordering and is therefore neglected in the following. From Eqs. (2) and (3) it is seen that, in general, $\sigma(n) = \sigma_0 n^{p_\rho}$ where p_ρ is a parameter determined by the scattering mechanism: $p_\rho = \frac{2}{3}$ and 2 for acoustic and impurity scattering, respectively. Since $\sigma(T)$ data exist for all samples, $\sigma(n)$ can be extracted at all temperatures. The parameter $p_\rho(T)$ can be determined by fitting a linear function to $\ln\sigma(n) = \ln\sigma_0 + p_\rho \ln n$. A linear relationship between $\ln\sigma(n)$ and $\ln n$ is only expected if one scattering mechanism dominates the resistivity. As an example the inset of Fig. 4 shows $\ln\sigma(n)$ as function of $\ln n$ at 110 K. The solid lines represent linear fits where $p_\rho = 1.25$ and 0.74 for the α and β samples, respectively. The fitting procedure has been done in the whole temperature range, and the result can be seen in Fig. 4 where $p_\rho(T)$ is plotted. For the α samples, p_ρ has a large temperature dependence; the exponent decreases from ~1.8 at 2 K to ~1.0 at 400 K. This indicates that at low temperatures ρ is dominated by scattering from impurities and that at high temperatures phonon scattering starts to contribute. This is in agreement with the observation that RRR decreases with increasing ρ(2 K) [Fig. 1(a)], since impurity scattering increases for low n relative to phonon scattering, as seen from Eqs. (2) and (3). For the β samples $p_\rho(T)$ is

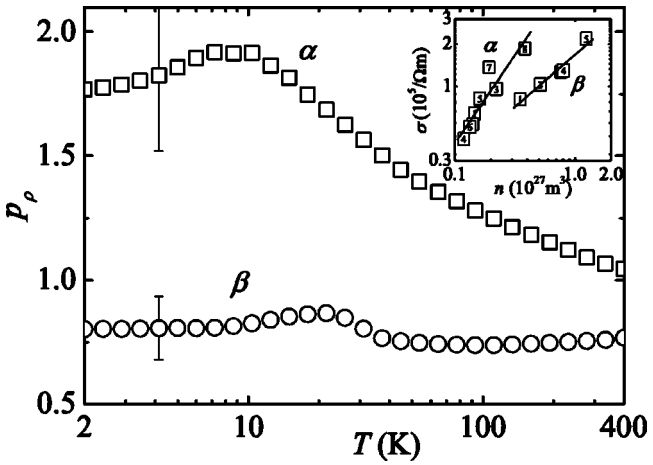

FIG. 4. Scattering parameter (p_ρ) as function of temperature (T) as obtained from fitting $\ln\sigma(n)=\ln\sigma_0+p_\rho\ln n$ for the α-$Eu_8Ga_{16-x}Ge_{30+x}$ samples (squares) and β-$Eu_8Ga_{16-x}Ge_{30+x}$ samples (circles), where σ is the electrical conductivity, n the carrier concentration and σ_0 a fit parameter. Error bars are representative for all data points. Inset shows σ for the α- and β-$Eu_8Ga_{16-x}Ge_{30+x}$ samples as function of n at 110 K. Solid lines are fits to data. See text for further explanation.

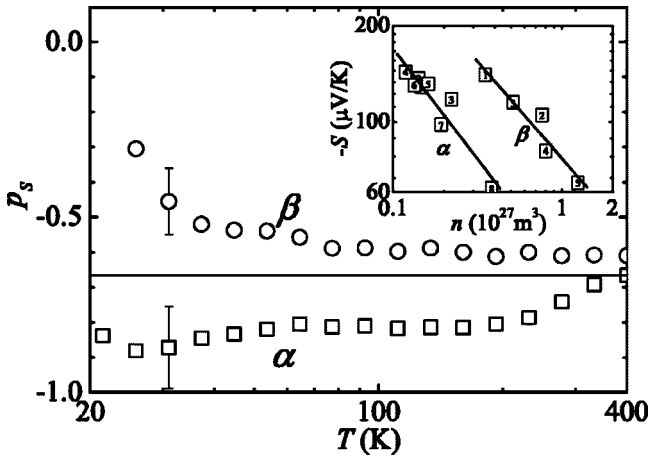

FIG. 5. Scattering parameter (p_S) as function of temperature (T) as obtained from fitting $\ln S(n)=\ln S_0+p_S\ln n$ for the α-$Eu_8Ga_{16-x}Ge_{30+x}$ samples (squares) and β-$Eu_8Ga_{16-x}Ge_{30+x}$ samples (circles), where S is the thermopower, n the carrier concentration and S_0 a fit parameter. Error bars are representative for all data points. The solid line represents $-2/3$. Inset shows S for the α- and β-$Eu_8Ga_{16-x}Ge_{30+x}$ samples as function of n at 333 K. Solid lines are fits to data. See text for further explanation.

very close to $\frac{2}{3}$ at high temperatures, as expected if phonon scattering is present only. This agrees well with the observation that RRR is almost constant among the β samples (Fig. 1(b)). As the temperature decreases, $p_\rho(T)$ increases slightly but stays quite far from the ideal value of 2 expected if impurity scattering dominates. For the α samples impurity scattering dominates in a large temperature range and l_e is therefore dependent on n. For $\alpha 4$, l_e decreases from 22 Å at 2 K to 19 Å at 300 K and, for $\alpha 8$, l_e is 83 Å and 32 Å at 2 K and 300 K, respectively. For the β samples phonon scattering dominates at high temperatures, which leads to a l_e independent of n and at 300 K, l_e is approximately 15 Å for all β samples. From Table I it is seen that, even at 2 K, l_e only shows a small variation with n. It is emphasized that the calculated l_e is based on $A=1$. If the theoretical A is used l_e increases by a factor $A^{-2/3}$. In any case, l_e is extremely low when compared to phosphorus doped Si with comparable n, where $l_e\sim 100$ Å at 300 K.[25]

A similar analysis for $S(T,n)$ is possible. The Mott relation

$$S=\frac{\pi^2k_B^2T}{3e}\left[\frac{\partial\ln(\sigma(\varepsilon))}{\partial\varepsilon}\right]_{\varepsilon=\varepsilon_F} \tag{4}$$

is used as starting point. Using Eq. (1), $A=1$ and the free-electron model relation between ε and n, Eq. (4) takes the form

$$S=\frac{2\pi^2k_B^2m^*T}{3e\hbar^2}\frac{(r+3/2)}{(3\pi^2n)^{2/3}}, \tag{5}$$

where r is the exponent in $\tau=\tau_0\varepsilon^r$. Provided that one scattering mechanism dominates, the thermopower has the form $S(n)=S_0n^{p_S}$ with $p_S=-\frac{2}{3}$, independent of the scattering mechanism. As before, it is possible to evaluate $p_S(T)$ by fitting a linear function to $\ln S(n)=\ln S_0+p_S\ln n$ at different temperatures. The result is seen in Fig. 5 where $p_S(T)$ is plotted for the α and β samples, respectively. Since $S(T)$ is poorly determined at low temperatures, only data above 20 K have been used. The inset is an example of $\ln S(n)$ as function of $\ln n$ at 333 K, the solid lines are linear fits with $p_S=-0.51$ and -0.61 for the α and β samples, respectively. For the α samples $p_S(T)$ increases from -0.85 at 20 K to -0.65 at 400 K. This agrees with $p_\rho(T)$, which showed that ρ at 20 K is mostly determined by impurity scattering but with contributions from phonon scattering. As the temperature increase phonon scattering starts to dominate at high temperature and $p_S(T)$ approaches the value $-\frac{2}{3}$. This is expected if only one scattering mechanism is present. For the β samples $p_S(T)$ decreases from approximately -0.3 at 25 K to approximately -0.55 at 50 K. Above this temperature $p_S(T)$ approaches the value $-\frac{2}{3}$ as the temperature increases. However, at low temperatures where impurity scattering dominates, p_S is quite far from $-\frac{2}{3}$. It is probably not a coincidence that at low temperatures both p_S and p_ρ for the β samples fall outside the expectations from the rigid-band model. Whether this is due to a failure of the parabolic band assumption in the free-electron model or some other effect is not clear.

When one scattering mechanism dominates, m^* can be estimated from S and n as seen from Eq. (5). In the following the abbreviation m_B^* will be used for an effective mass derived from S and n to emphasize that it is the band effective mass. In Table I, m_B^* is calculated for all samples assuming phonon scattering and using $S(400\text{ K})$. For the α samples this leads to $m_B^*\approx 1.5m_0$, where m_0 is the free-electron mass. However, for the α samples more than one scattering mechanism is present at almost all temperatures. Therefore we also calculated m_B^* from $S(45\text{ K})$ with the assumption that impu-

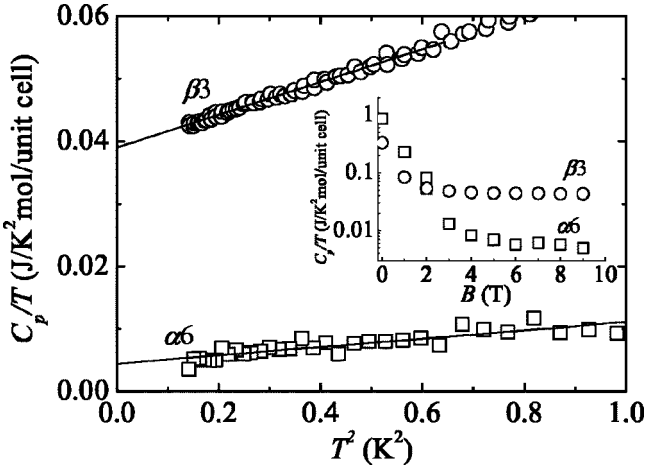

FIG. 6. Specific heat to temperature ratio ($C_p(T)/T$) as function of T^2 for α6 (squares) and β3 (circles) measured in a 9 T magnetic field. Inset shows $C_p(T)/T$ as function of magnetic field (B) measured at 0.4 K.

rity scattering dominates. This leads to $m_B^* \approx 0.8m_0$ which is a factor of two smaller than m_B^* if phonon scattering is assumed. Thus, we obtain that $m_B^* \approx m_0$ for the α samples. In the β samples phonon scattering dominates at high temperatures and the average m_B^* is $\sim 3.2m_0$ for all samples calculated with S(400 K). Using S at temperatures down to 200 K changes m_B^* only slightly.

To investigate the differences in m^* for the α and β phase in detail, low-temperature $C_p(T)$ has been measured for sample α6 and β3. The result is plotted in Fig. 6 as C_p/T vs T^2. The straight lines correspond to fits with the relation $C_p/T = \gamma + \beta T^2$, where the Sommerfeld coefficient γ represents the electronic contribution and the βT^2 term the phononic contribution with $\beta = 12\pi^4 NR/(5\theta_D^3)$. N and R are the concentration of atoms and the gas constant, respectively. In order to suppress contributions from the magnetic ordering $C_p(T)$ was measured in a 9 T magnetic field. The magnitude of γ confirms that m^* is larger in the β structure than in the α structure. Dependent on whether a normal or spin polarized free-electron model is used, the density of states effective masses (m_{DOS}^*) are calculated to be $0.75m_0$ ($1.2m_0$) and $4.6m_0$ ($6.3m_0$) for the α6 and β3 sample, respectively. The numbers in brackets are for the spin-polarized free-electron model. The inset of Fig. 6 shows the change of C_p/T as function of magnetic field at 0.4 K. Even at the largest magnetic field of 9 T, C_p/T still decreases with increasing field. It can, therefore, not be excluded that the magnetic ordering still contributes to C_p/T and that m_{DOS}^* and the density of states are slightly overestimated. Θ_D calculated from β gives 251 and 159 K for α6 and β3, respectively. Especially for the β sample this value is lower than previously published values.[8] It could be argued that this extra specific heat is due to the presence of either localized Einstein vibrational modes or low-energy excitations related to tunneling states. However, the Einstein temperature has to be as low as 12 K to make such a large contribution to $C_p < 1$ K and a clear exponential increase of C_p/T with increasing temperature would, in any case, be expected. A measurement of $C_p(T)$ on $Sr_8Ga_{16}Ge_{30}$ (not shown), which has very similar thermal transport properties to β-$Eu_8Ga_{16}Ge_{30}$, shows no extra specific heat and $\beta(\Theta_D)$ is similar to what is observed for α6. Thus, tunneling states cannot be the source of the extra specific heat. Although it would be expected that the phase with the lowest ordering temperature (α phase) has the largest contribution to C_p at lowest temperatures we nevertheless conclude that the magnetic contribution is responsible for the extra specific heat in β3.

Kuznetsov *et al.*[7] found similar values for m_B^*. For $Ba_8Ga_{16}Sn_{30}$ (type VIII structure), $m_B^* = 0.9m_0$, and for $Sr_8Ga_{16}Ge_{30}$, $m_B^* = 3.0m_0$. Uher *et al.*[26] have measured both S and n of two $Sr_8Ga_{16}Ge_{30}$ samples which we combine to $m_B^* = 3.9m_0$ and $4.7m_0$. Sales *et al.*[20] found $m_B^* \sim 3m_0$, for $(Sr/Ba/Eu)_8Ga_{16}Ge_{30}$. Thus the differences in m_B^* appear to be related to the structure and are almost independent of n. This is supported by recent band structure calculations[13] that predict an enhanced S (that is, a large m_B^*) for $(Sr/Eu)_8Ga_{16}Ge_{30}$ compared to α-$Eu_8Ga_{16}Ge_{30}$. As before it is emphasized that in all calculations a Hall scattering factor of unity has been used.

Since l_e is several orders of magnitude lower than the average grain size, it can be excluded that grain boundary scattering has an influence on the transport properties. At the same time it seems unlikely that the small amount of foreign phases, which cannot be detected by x-ray diffraction but only by energy dispersive x-ray spectroscopy,[15] is responsible for the observed transport properties. This is also supported by the fact that the temperature dependence of ρ and the RRR of β5 is similar to that of the single crystalline β-$Eu_8Ga_{16}Ge_{30}$ sample in Refs. 19 and 20. The origin of the large impurity scattering must, therefore, be intrinsic and is probably related to either the ionically bonded cations, the random positioning of Ga/Ge or a combination of both. From Eqs. (2) and (3) it is seen that a low n increases impurity scattering relative to phonon scattering. Since the α samples have an overall lower n than the β samples, this could be the reason why impurity scattering apparently is larger in the α samples than in the β samples.

Figure 7 shows ZT as function of n at 193 and 400 K for all the samples presented in this report. κ(400 K) is estimated by adding κ_e, calculated from the Wiedemann-Franz law, to an estimated $\kappa_L(400\ \mathrm{K}) = 0.85$ W/mK. Literature data suggests that κ_L of β-$Eu_8Ga_{16}Ge_{30}$ above 200 K is constant.[20] For the α samples ZT is almost constant at ~ 0.1 and ~ 0.35 at 193 K and 400 K, respectively. For the β samples ZT increases as n decreases. The sample with lowest n (β1) reaches $ZT \approx 0.4$ at 400 K.

In the temperature range from 200 to 400 K, the simple dependence of the transport properties on n for the β phase allows an extrapolation of the thermoelectric properties to lower n. σ can be extrapolated by $\sigma(n) = \sigma_0 n^{p_\rho}$ where the fitted σ_0 and $p_\rho = \frac{2}{3}$ is used, and S is extrapolated by $S(n) = S_0 n^{p_S}$ where the fitted S_0 and $p_S = -\frac{2}{3}$ is used. κ_L is again assumed to be constant at 0.85 W/Km, and κ_e is calculated from the Wiedeman-Franz law. For the α samples an extrapolation has not been attempted because of the combined impurity and phonon scattering in the whole temperature range. The results of the extrapolations can be seen in Fig. 7

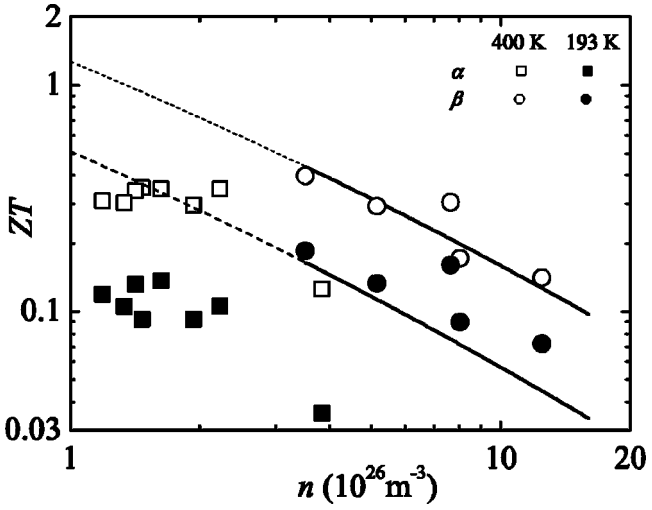

FIG. 7. The measured dimensionless figure of merit ($ZT = S^2T\sigma/\kappa$, where S is the thermopower, σ the electrical conductivity, κ the thermal conductivity, and T the temperature) for the β-$Eu_8Ga_{16-x}Ge_{30+x}$ samples (open circles 400 K, solid circles 193 K) and α-$Eu_8Ga_{16-x}Ge_{30+x}$ samples (open squares 400 K, solid squares 193 K) as function of carrier concentration (n). Solid lines are ZT calculated from the parabolic rigid-band model for β-$Eu_8Ga_{16}Ge_{30}$ at 193 K (lower line) and 400 K (upper line). Dashed lines are the same models extrapolated to lower n.

where $ZT(n)$ is plotted for 193 and 400 K. It is seen that the model tracks the data quite well and $ZT>1$ is reached for n lower than $1.4\times10^{26}e^-/m^3$ at 400 K. At this concentration and temperature $\rho=3750\ \mu\Omega$ cm, $S=317\ \mu$V/K, $\kappa_{tot}=1.07$ W/mK and $T_F=370$ K. In this extrapolation several effects have been neglected. First, it has been assumed that only phonon scattering is present. For the α samples the small variation of ZT with n is due to the combined phonon and impurity scattering, and Fig. 7 suggests that if lower n can be obtained for the β phase, then an increase in the impurity scattering could be expected and ZT vs n would level out as seen for the α samples. Second, it has been assumed that the charge carriers are degenerate. This is not the case when $T_F=370$ K, and for $T\sim T_F$ there is no longer a simple power-law dependence of σ and S on n. A more detailed calculation reveals that the extrapolation overestimates ZT. Therefore it is doubtful if $ZT>0.5$ around room temperature, for n-type clathrates with divalent cations, can be reached without modifications enhancing the thermoelectric properties, e.g., enhancement of S by the Kondo effect. However, for $T>T_F$ the exponents p_ρ and p_S take the values 1 and −1, respectively, and ZT increases more rapidly with decreasing n than for $T<T_F$. This suggests that the clathrates may have a potential for high-temperature power generation where the relatively large band gaps ensure that intrinsic carriers are not excited from the valence band into the conduction band.

IV. PHONON TRANSPORT

The glasslike $\kappa_L(T)$ of $(Sr/Eu)_8Ga_{16}Ge_{30}$ has previously been explained by a combination of resonant scattering of phonons from the cations and scattering of phonons from cation tunneling states.[19,20,27,28] This interpretation is supported by the thermal displacement factors extracted from diffraction experiments, which, for the Eu and Sr atoms on the $\frac{1}{4}\ \frac{1}{2}\ 0$ site in the type I structure, are extremely large. The diffraction data are better modeled if the Eu and Sr atoms on this position are allowed to be positioned slightly off center, at four split positions.[8,20,29] It is, therefore, straightforward to believe that the low-energy excitations arise from tunneling between the different equilibrium positions. The thermal displacement factors for Eu in the α phase are, although large, smaller than in the type I structure.[8] This may indicate that less or no tunneling states are present and thus explain the differences in κ_L at low temperatures between α-$Eu_8Ga_{16}Ge_{30}$ and $(Sr/Eu)_8Ga_{16}Ge_{30}$. However, it has been shown that the cations even in $Ba_8Ga_{16}Si_{30}$ (Ref. 30) and $Ba_8Ga_{16}Ge_{30}$ (n-type)[31] are not located in the center of the cages, but these compounds do not possess a glasslike κ_L. At the same time it would be expected that simple disorder with four split positions would result in a highly localized density of tunneling states leading to a κ_L similar to what is observed for resonant scattering. In a recent publication[14] it was shown that p-type $Ba_8Ga_{16}Ge_{30}$, unlike n-type $Ba_8Ga_{16}Ge_{30}$, has a glasslike κ_L. Unless the density of tunneling states is sample dependent, this result is in conflict with the tunneling states model and suggests that the charge carriers play an important role. Finally, ultrasonic attenuation (UA) measurements on $Sr_8Ga_{16}Ge_{30}$ (Refs. 28 and 32) give a density of tunneling states lower than observed for glasses and estimates of $\kappa_L(T)$ from the UA measurements leads to a κ_L which is an order of magnitude larger than observed,[33] indicating that scattering from tunneling states is of minor importance. Recently also a four-well tunneling states model for the Eu atoms in the large cages was proposed.[34] However, this model predicts an upturn in the specific heat below approximately 0.8 K that is not observed experimentally (Fig. 6). Furthermore, this model gives a localized density of tunneling states, which again cannot lead to a power-law dependence of the lattice thermal conductivity on temperature. In another recent paper[35] it is proposed that the glasslike low-temperature κ_L of $(Sr/Eu)_8Ga_{16}Ge_{30}$ is determined by an impurity-like scattering mechanism due to the off-center position of the cations being absent for $Ba_8Ga_{16}Ge_{30}$ and thereby explaining the "normal" κ_L of $Ba_8Ga_{16}Ge_{30}$. However this model cannot explain the glasslike κ_L of p-type $Ba_8Ga_{16}Ge_{30}$,[14] which has identical crystal structure and displacement of the cation when compared to the n-type. Instead, we suggest that phonon-charge-carrier scattering should be considered when describing κ_L at the lowest temperatures. As will be seen later in this section, this model can account for differences in the low-temperature κ_L, not only among α- and β-$Eu_8Ga_{16-x}Ge_{30+x}$ samples, respectively, but also for the large difference in κ_L between the α and β phase. The difference in κ_L at intermediate and high temperatures both among α- and β-$Eu_8Ga_{16-x}Ge_{30+x}$ samples and between the α and β phase is interpreted as differences in the coupling between the resonant scatterers and the heat-carrying acoustic phonons. It is suggested that the coupling is closely related to the electronic band structure. The rest of the section is out-

lined as follows. First, different phonon-charge-carrier scattering models are discussed. This is followed by a quantitative modeling of $\kappa_L(T)$ for $\alpha 7$ and $\beta 1$ samples considering phonon-charge-carrier scattering in combination with the usual resonant and Rayleigh scattering. Then we discuss the differences in $\kappa_L(T)$ among the α- and β-$Eu_8Ga_{16-x}Ge_{30+x}$ samples and between the α and β phase, respectively, and finally we review $\kappa_L(T)$ data for $Sr_8Ga_{16-x}Ge_{30+x}$.

In electrically conductive solids phonon-charge-carrier scattering can have a strong impact on the magnitude and temperature dependence of κ_L. In elemental Ge, with slightly lower n than in the samples presented in this paper, phonon-charge-carrier scattering can reduce κ_L to as low a value as 1 W/(Km) at 2 K,[36] which is of the same order of magnitude as κ_L(2 K) of the α and β samples. It was shown by Ziman[23,37] that scattering of acoustic phonons from free degenerate carriers can, to a good approximation, be regarded as impossible for phonons with a wave number (q) larger than $2k_F$, where k_F is the Fermi wave number. In the dominant phonon approximation this corresponds to a characteristic temperature $T^* \simeq 2k_F\hbar v_p/(3.8k_B)$, where v_p is the speed of sound. For the samples presented in this report $T^* \simeq 20-40$ K. $\kappa_L(T)$ due to phonon-charge-carrier scattering (κ_{p-e}) below T^* is proportional to T^2. Above T^*, κ_{p-e} increases rapidly with temperature and is negligible if other scattering mechanisms are present. The magnitude of κ_{p-e} is proportional to $1/(\varepsilon_{\rm def}^2 \times m^{*2})$, where $\varepsilon_{\rm def}$ is the deformation potential and defines the strength of the phonon-charge-carrier coupling. If this model is fitted to $\kappa_L(T)$, then reasonable values of $\varepsilon_{\rm def}$ are obtained and the large difference in κ_L between α and β samples at the lowest temperatures can be explained by m^*, which is at least three times larger for the β phase than for the α phase. However, the Ziman model is only valid for $ql_e \gg 1$. This is not fulfilled for the samples in the present study: depending on the sample the extremely low l_e leads to $ql_e(2\ {\rm K}) \simeq 1-3$. Pippards ineffectiveness condition states that the phonon-charge-carrier relaxation time increases with decreasing l_e when $ql_e < 1$.[23,38] This contradicts the observation that κ_L of the α samples increases with increasing l_e (see inset of Fig. 8). However, the generality of the Pippards ineffectiveness condition has recently been challenged by the authors of Ref. 39. It is argued that in disordered or impure materials a fraction of the charge-carrier scattering associated with the mean-free path L_e, occurs on scatterers that do not vibrate with the lattice. It is shown that the phonon-charge-carrier scattering rate increases, as opposed to the Pippard model, as L_e decreases when $ql_e < 1$. It was earlier argued that the low l_e was due to either the cations or disorder on the Ga/Ge sites. Since the vibration of the cations usually are described as Einstein oscillators these are the most obvious candidates for scatterers that do not vibrate with the lattice.

A. Modeling of κ_L for $\alpha 7$ and $\beta 1$

According to Ref. 39, the inverse mean-free path of longitudinal and transverse phonons scattered on charge carriers is

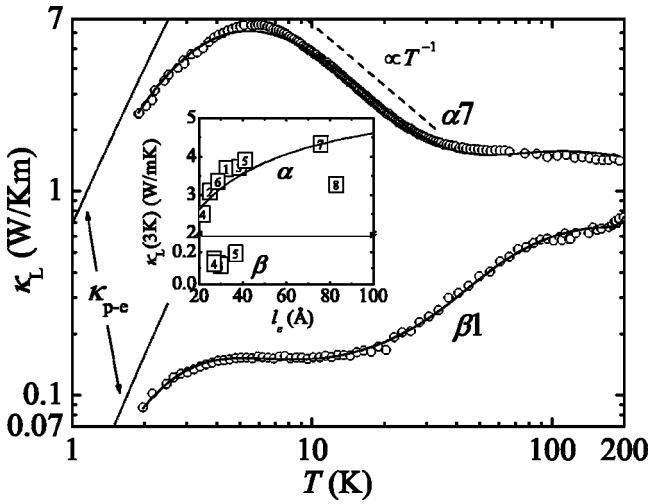

FIG. 8. Lattice thermal conductivity (κ_L) as function of temperature (T) for $\alpha 7$ and $\beta 1$. Solid lines are fits to a model described in text. Dotted lines (κ_{p-e}) are the lattice thermal conductivity in this model if phonon-charge-carrier scattering is present only. Inset shows κ_L(3 K) as function of the mean-free path of the charge carriers (l_e) of the α- and β-$Eu_8Ga_{16}Ge_{30}$ samples.

$$l_{p-e,l}^{-1}(q) = 2Bq\frac{v_p}{v_F}\left[\frac{ql_e\arctan(ql_e)}{ql_e - \arctan(ql_e)} - \left(1-\frac{l_e}{L_e}\right)\frac{3}{ql_e}\right]P(z) \tag{6}$$

$$l_{p-e,t}^{-1}(q) = 6B\frac{v_p}{l_e v_F}\left(1-\frac{l_e}{L_e}\right)\left[1+\left(1-\frac{l_e}{L_e}\right)\times\frac{3ql_e - 3(ql_e)^2\arctan(ql_e) - 3\arctan(ql_e)}{2(ql_e)^3}\right]P(z), \tag{7}$$

where $B=(2\varepsilon_F/3)^2 m^* p_F/(2\pi^2 D_m v_p^2 \hbar^3)$, p_F is the Fermi momentum and D_m is the mass density. It has been assumed that the longitudinal and transverse phonon speed is the same. Inserting the free-electron model value of p_F and making the substitution $2\varepsilon_F/3 \rightarrow \varepsilon_{\rm def}$ (Ref. 23) leads to $B = \varepsilon_{\rm def}^2 m^{*2}/(2\pi^2 D_m v_p^2 \hbar^3)$. In the limit $ql_e \gg 1$ and $L_e \gg l_e$, Eq. (6) correctly reproduces the Ziman equation.[23,37] In the limit $L_e \gg l_e$ both Eqs. (6) and (7) reproduce the functional dependence of the phonon-electron scattering rate on ql_e of the Pippard theory.[38,39] $P(z)$ is a cutoff function that only allows phonons with $q < 2k_F$ to be scattered.[37] $\kappa_L(T)$ calculated from Eqs. (6) and (7) results in $\kappa_L \propto T^p$, where p can have approximate values between 1 and 2 for a wide range of ql_e and l_e/L_e values.

Earlier $\kappa_L(T)$ for $Eu_8Ga_{16}Ge_{30}$ and $Sr_8Ga_{16}Ge_{30}$ has been fitted to a model where tunneling states and resonant and Rayleigh scattering have been included.[8,19,27] Here we replace the tunneling term with a phonon-charge-carrier scattering term and the total phonon mean-free path beomes

$$l_p = \tfrac{1}{3}(l_{p-e,l}^{-1} + l_{\rm res}^{-1} + l_R^{-1} + l_C^{-1})^{-1} + \tfrac{2}{3}(l_{p-e,t}^{-1} + l_{\rm res}^{-1} + l_R^{-1} + l_C^{-1})^{-1} + l_{\rm min}, \tag{8}$$

where $l_R^{-1} = D(zT)^4$, l_C is the Casimir mean-free path,

$$l_{\mathrm{res}}^{-1}(z) = \sum_i \frac{C_{\mathrm{res},i}(\hbar z T^2/k_B)^2}{[\Theta_{E,i}^2 - (zT)^2]^2 + \gamma_i \Theta_{\mathrm{E},i}^2 (zT)^2} \tag{9}$$

and $C_{\mathrm{res},i}$, γ_i and D have their usual definition.[19] Because of the different scattering rates for the phonon-charge-carrier scattering it is necessary to separate l_p into contributions from longitudinal and transverse phonons as is seen from Eq. (8).

$C_p(T)$ calculated from Θ_D combined with $\kappa_L(2\ \mathrm{K})$ gives an estimate for $l_p(2\ \mathrm{K})$ of the order of 1000 μm for the α samples and 30 μm for the β samples. The grain sizes in the α- and β-$Eu_8Ga_{16-x}Ge_{30+x}$ samples studied in this paper are of the order of 10–100 μm and 200–400 μm for the α and β phase, respectively.[15] Thus, in the case of the β phase the effect of grain boundary scattering can *a priori* be neglected. For the α phase it cannot be excluded that grain boundary scattering has an influence on the thermal resistivity. However, it is clear that if l_C was of the same size as the grain size, κ_L would be much lower than observed. This indicates that grain boundary scattering has little influence also for the α phase. In the subsequent modeling of κ_L it is assumed that only sample boundary scattering exists and that l_C can be calculated from the sample size. In any case excluding l_C from the modeling only affects the value of the other fitted parameters little and this justifies even a large error in l_C. All samples have an approximate cross section (CS) of 2 mm^2, leading to $l_C = \sqrt{4CS/\pi} = 1600$ μm.

The lattice thermal conductivity is then expressed as[40]

$$\kappa_L(T) = v_p/3 \int_0^{\Theta_D/T} C(T,z) \cdot l(T,z) dz, \tag{10}$$

with B, l_e/L_e, $C_{\mathrm{res},i}$, γ_i, D, and l_{min} as fit parameters.

For the modeling of $\kappa_L(T)$ we used $\Theta_E = 72$ K for the α samples and $\Theta_{E1} = 75$ K and $\Theta_{E2} = 45$ K for the β samples.[8] The parameters Θ_D, v_p, D_m,[8] l_e, m^* are also kept constant at their experimentally determined values. At low temperatures l_e varies slowly with temperature and $l_e(2\ \mathrm{K})$ was used. To minimize the number of fit parameters it is assumed that for the β samples $\gamma_1 = \gamma_2$ and $\frac{1}{4}C_{\mathrm{res},1} = \frac{3}{4}C_{\mathrm{res},2}$, which reflects the relative amounts of Eu on the 000 and $\frac{1}{4}\ \frac{1}{2}\ 0$ sites. For the α samples l_{min} was refined to unphysical values because of correlations with γ and D and was, subsequently, kept at the arbitrary value 2.2 Å. The value of l_{min} does not affect the fits at low temperatures. The parameters B and l_e/L_e were initially allowed to vary freely and good fits were obtained. However, due to correlations this resulted in a large variation of B and l_e/L_e from sample to sample and therefore the value of l_e/L_e was constrained arbitrarily to 0.7.

Figure 8 shows the result of the modeling of $\kappa_L(T)$ for the $\alpha 7$ and $\beta 1$ sample. For $\alpha 7$, $B = 6.3 \times 10^{-4}$, $C_{\mathrm{res}} = 2.2 \times 10^{30}\ \mathrm{m}^{-1}\ \mathrm{K}^{-2}\ \mathrm{s}^{-2}$, $\gamma = 0.47$, $D = 0.39\ \mathrm{m}^{-1}\ \mathrm{K}^{-4}$. For $\beta 1$, $B = 7.2 \times 10^{-3}$, $C_{\mathrm{res}} = 6.7 \times 10^{31}\ \mathrm{m}^{-1}\ \mathrm{K}^{-2}\ \mathrm{s}^{-2}$, $\gamma = 5.1$, $D = 2.7\ \mathrm{m}^{-1}\ \mathrm{K}^{-4}$, and $l_{\mathrm{min}} = 3.4$ Å. For $\alpha 7$ there is a small difference between the fit and the data around 7 K. This could be attributed to neglecting the temperature dependence of l_e and/or l_e/L_e. It is noted that the $\kappa_L \propto T^{-1}$ dependence of α-$Eu_8Ga_{16-x}Ge_{30+x}$ in the range 10–40 K is described well by resonant scattering, while in the literature it has been interpreted as a sign of anharmonic phonon-phonon umklapp scattering.[19]

The parameters C_{res}, γ, D, and l_{min} are representative for all samples and are in agreement with the values obtained in previous studies.[8,16,19,27] If it is assumed that Ga and Ge are randomly positioned, the theoretical value of D due to mass difference and isotope scattering[23] is $0.00285\ \mathrm{m}^{-1}\ \mathrm{K}^{-4}$ and $0.00554\ \mathrm{m}^{-1}\ \mathrm{K}^{-4}$ for α- and β-$Eu_8Ga_{16}Ge_{30}$, respectively. v_p of Ref. 8 is used in the calculation. This value is about three orders of magnitude lower than the fitted value which indicates that this type of scattering has little influence on $\kappa_L(T)$. For glasses, D is typically $100-1000\ \mathrm{m}^{-1}\ \mathrm{K}^{-4}$,[41] and much higher than the fitted value. If the term is left out of the modeling, then $\kappa_L(T)$ above approximately 70 K is fitted poorly because the resonance term leads to a wavy feature in $\kappa_L(T)$ at temperatures around $0.4\Theta_E - 0.9\Theta_E$. This effect can be seen from the modeling of $\kappa_L(T)$ for $\alpha 7$ in Fig. 8 just above 30 K. The Rayleigh term results in a constant κ_L above approximately 50 K, smoothing out the wavy feature, and we believe that the large D can be interpreted as a compensation for errors in the assumptions of the resonance scattering model. We base this on the following arguments. Each vibrational mode of the Eu atoms should be treated independently. If the off-center position of Eu2 in β-$Eu_8Ga_{16}Ge_{30}$ is neglected, then Eu1 and Eu2 have one and two independent vibrational modes, respectively. If a C_{res}, Θ_E, and γ is assigned to each mode, then this gives a total of nine parameters, which can lead to a broadening of the resonance scattering and a smoothed out $\kappa_L(T)$. The single Eu site in α-$Eu_8Ga_{16}Ge_{30}$ has high symmetry,[8] and there is, in principle, only one independent vibrational mode. However, the thermal displacement factors of Eu are large,[8] indicating that the Eu atoms are not located in the center of the cage. Together with the random positioning of Ga/Ge, which changes the local Eu bonding environment, this lowers the symmetry and increases the number of independent modes that are necessary to obtain a smooth $\kappa_L(T)$. It is noted that Eq. (9) is an empirical model.[42] A theoretically founded model was developed in Ref. 43, but this also leads to wavy features in $\kappa_L(T)$ around $0.4\Theta_E - 0.9\Theta_E$.

B. The differences in κ_L among α- and β-$Eu_8Ga_{16-x}Ge_{30+x}$ samples

For both the α and β samples there is a tendency for C_{res} and D to decrease and B to increase with increasing n (not shown). The decrease of C_{res} and D shows that the resonance scattering rate decreases with increasing n and a possible explanation could be that the conduction electrons screen the resonant scattering cations. The screening becomes more effective for larger n and reduces the coupling between the phonons and the vibration of the cations. On the other hand, band structure calculations have shown that the conduction bands arise from both cation and antibonding framework states.[13] The change of the coupling could then be a result of changes in the bonding of the cations to the framework as n changes. The increase of B with increasing n is expected because $\varepsilon_{\mathrm{def}}$ increases with increasing n. $\varepsilon_{\mathrm{def}}$ can be calculated from $B = \varepsilon_{\mathrm{def}}^2 m^{*2}/(2\pi^2 D_m v_p^2 \hbar^3)$ to be in the range from

0.25 to 0.5 eV for all samples. For *p*-type InSb with slightly lower n, ε_{def} determined from $\kappa_L(T)$ is of the order 1.0 eV,[44] which is of the same magnitude as ε_{def} of the clathrates. This shows that phonon-electron scattering cannot be neglected.

To emphasize that phonon-charge-carrier scattering can explain κ_L at low temperatures, $\kappa_L(3\text{ K})$ has been calculated as function of l_e for the α phase and the result is plotted as the solid curve in the inset of Fig. 8. The only adjustable parameter is l_e. The other parameters were kept constant at the values that were fitted for $\alpha 7$ with the assumption that $l_e/L_e=0.7$. It is seen that, with the exception of $\kappa_L(3\text{ K})$ for $\alpha 8$, the model tracks the data quite well, and it can be concluded that the variation of κ_L at 3 K among different samples is dominated by the variation of l_e. For the β samples the variation of κ_L is much smaller because l_e only varies little. It is emphasized that the Pippard model[38] leads to a decreasing κ_L as l_e increases, in clear disagreement with our findings.

C. The difference in κ_L between the α and β phase

As mentioned earlier the large difference in κ_L at low temperatures, between α- and β-$Eu_8Ga_{16}Ge_{30}$, is a result of different values of m^*, because $\kappa_{p-e} \propto 1/m^{*2}$. As can be seen from Fig. 8 phonon-charge-carrier scattering has a vanishingly small contribution to $\kappa_L > 10$ K and the differences in κ_L between the α and β phase originate from differences in the resonance scattering. From the fitting of $\kappa_L(T)$, C_{res} was found to be $\sim$20 times larger in the β samples than in the α samples. It can only be speculated about the large difference in the coupling, but the band structure and charge carries appear to have a large indirect influence on the coupling. In a recent publication[14] it was shown that *n*-type $Ba_8Ga_{16-x}Ge_{30+x}$ samples have a "normal" $\kappa_L(T)$, while *p*-type $Ba_8Ga_{16-x}Ge_{30+x}$ samples have a glasslike $\kappa_L(T)$; that is, the resonance scattering and coupling is enhanced in the latter. This correlates with m^*; which is approximately twice as large for *p*-type than for *n*-type $Ba_8Ga_{16-x}Ge_{30+x}$. For α- and β-$Eu_8Ga_{16-x}Ge_{16+x}$ the same tendency is observed. The α phase has $m^* \simeq m_0$ and a normal κ_L, while the β phase has $m^* > 3m_0$ and a glasslike κ_L. The fact that β-$Eu_8Ga_{16-x}Ge_{30+x}$, $Sr_8Ga_{16-x}Ge_{30+x}$ and *p*-type $Ba_8Ga_{16-x}Ge_{30+x}$, which are the only clathrate samples in the literature that have $m^* > 3m_0$, are also the ones with a glasslike κ_L supports this idea. Band structure calculations[13] predict that m^* of the charge carriers in the valence band of α-$Eu_8Ga_{16-x}Ge_{30+x}$ are enhanced compared to those in the conduction band. If *p*-type α-$Eu_8Ga_{16-x}Ge_{30+x}$ could be synthesized then this would be a possibility to test our empirical model, which predicts that *p*-type α-$Eu_8Ga_{16-x}Ge_{30+x}$ has a glasslike κ_L.

The effect of a magnetic field on κ_L was investigated by measuring $\kappa_L(B)$ at 2, 5, and 10 K in magnetic fields up to 9 T and by measuring $\kappa_L(T)$ in 0 and 9 T for the $\alpha 2$ and $\beta 1$ samples (not shown). For $\alpha 2$ there is a tendency for κ_L to increase slightly with field. For the $\beta 1$ sample no change within the resolution of the equipment ($<3\%$) was observed, in agreement with Ref. 20. Thus, the relaxation time related to the scattering on magnetic moments is very large compared to the dominant scattering mechanism. Furthermore, it can be concluded that magnons do not contribute significantly to the thermal transport, which excludes that the peak in κ_L for the α samples is related to the magnetic ordering at approximately the same temperature.

D. κ_L of $Sr_8Ga_{16-x}Ge_{30+x}$

κ_L of $Sr_8Ga_{16-x}Ge_{30+x}$ has been intensively studied. To the authors knowledge eight different samples have been investigated in the literature.[4,7,19,20,26,27] The "sintered" sample of Ref. 26 is not included in the following discussion since it is obvious from $\rho(T)$ and $\kappa(T)$ that the transport properties are dominated by grain boundary scattering. As mentioned earlier m^* of *n*-type $Sr_8Ga_{16-x}Ge_{30+x}$ is in the range from $3m_0$ to $4.7m_0$ and similar to that of β-$Eu_8Ga_{16-x}Ge_{30+x}$. Like for $Ba_8Ga_{16-x}Ge_{30+x}$,[14] κ_L of $Sr_8Ga_{16-x}Ge_{30+x}$ is very sample dependent at temperatures below approximately 20 K. Unfortunately, n is only known exactly for two samples,[26,45] but the low-temperature κ_L values of different samples decrease with increasing ρ. Since, in general, $\rho \propto 1/(nl_e)$ this indicates that κ_L increases with increasing n and l_e, in agreement with the phonon-charge-carrier scattering model. It is particularly interesting to see that κ_L of the "quartz" sample, and to a lesser extent the PBN sample of Ref. 26, unlike other $Sr_8Ga_{16-x}Ge_{30+x}$ samples, have a peak at low temperatures. Comparing ρ of these two samples with literature values of other $Sr_8Ga_{16-x}Ge_{30+x}$ samples it is seen that ρ is low. Especially ρ of the quartz sample is anomalous, the residual resistance is below 0.025 mΩ cm and $\text{RRR}_{2-300\text{ K}}$ is close to 25, which is much larger than for any other $(\text{Ba/Sr/Eu})_8Ga_{16}Ge_{30}$ sample in the literature. Together, these result are consistent with phonon-electron scattering dominating the low-temperature κ_L. At temperatures above 30 K a clear resonance dip is seen for all samples and κ_L varies little. This shows that the resonance scattering is large and consistent with the large m^*.

V. CONCLUSION

In this paper it is shown that the varying transport properties of α- and β-$Eu_8Ga_{16-x}Ge_{30+x}$ can be described by a parabolic rigid-band model where $\varepsilon_F[n(x)]$ is the only varying parameter. In our companion paper,[15] we have shown that the carriers originate from a small deviation of the ideal Ga/Ge ratio. For the α phase $m^* \approx m_0$, while for the β phase $m^* > 3m_0$. These results are in agreement with recent band structure calculations[13] that predict larger m_B^* and m_{DOS}^* for *n*-type β-$Eu_8Ga_{16-x}Ge_{30+x}$ than for *n*-type α-$Eu_8Ga_{16-x}Ge_{30+x}$. The origin of the extremely low l_e is intrinsic and it is related to either the random positioning of Ga/Ge and/or to the presence of Eu^{2+} ions that scatter the charge carriers effectively. It, therefore, seems doubtful that any of the clathrates with divalent cations and randomly positioned framework atoms can be called a phonon glass electron crystal.[46] The charge carrier mobility (μ) of materials based on Bi_2Te_3,[47] $CsBi_4Te_6$,[1] and Zn_4Sb_3 (Ref. 3) is almost two orders of magnitude higher than the one of Tl_9BiTe_6 (Ref. 2) and type I and VIII clathrates with divalent cations.

The relatively good thermoelectric properties are due to an extremely low κ_L and large m^*. The analysis of the electric transport properties suggests that ZT at room temperature for n-type α- and β-$Eu_8Ga_{16-x}Ge_{30+x}$ will not exceed that of the best materials. However, because of the relative large m^* and ε_g there is reason to believe that β-$Eu_8Ga_{16-x}Ge_{30+x}$ has a potential for high-temperature power generation. It has been proposed that the low-temperature κ_L of clathrates can be explained by phonon-charge-carrier scattering, where a large m^* and a small l_e lead to an increased scattering rate. It has been shown that resonant scattering dominates κ_L above 10 K. The difference in κ_L between $(Sr/Eu)_8Ga_{16-x}Ge_{30+x}$ and p-type $Ba_8Ga_{16-x}Ge_{30+x}$ on one side, and n-type $Ba_8Ga_{16-x}Ge_{30+x}$ and α-$Eu_8Ga_{16-x}Ge_{30+x}$ on the other side is mainly determined by differences in the coupling of the resonant scatterers and the phonons. Very interestingly, this coupling correlates with m^*: a larger m^* leads to a larger coupling. Band structure calculations predict an enhanced m^* for p-type α-$Eu_8Ga_{16-x}Ge_{30+x}$.[13] According to our empirical model κ_L of this compound should be similar to the glasslike κ_L of $(Sr/Eu)_8Ga_{16-x}Ge_{30+x}$ and p-type $Ba_8Ga_{16-x}Ge_{30+x}$.

ACKNOWLEDGMENTS

We thank W. Carillo-Cabrera, M. Baenitz, and I. Zerec for fruitful discussions.

*Present address: Instituto de Física, Universidad Autónoma de Puebla, Apdo. Postal J-48, Puebla 72570, Mexico.
†Corresponding author. Email address: paschen@cpfs.mpg.de

[1] D. Chung, T. Hogan, P. Brazis, M. Rocci-Lane, C. Kannewurf, M. Bastea, C. Uher, and M. G. Kanatzidis, Science **287**, 1024 (2000).
[2] B. Wölfing, C. Kloc, J. Teubner, and E. Bucher, Phys. Rev. Lett. **86**, 4350 (2001).
[3] T. Caillat, J.-P. Fleurial, and A. Borshchevsky, J. Phys. Chem. Solids **58**, 1119 (1997).
[4] G. S. Nolas, J. L. Cohn, G. A. Slack, and S. B. Schujman, Appl. Phys. Lett. **73**, 178 (1998).
[5] P. S. Riseborough, Adv. Phys. **49**, 257 (2000).
[6] B. Eisenmann, H. Schäfer, and R. Zagler, J. Less-Common Met. **118**, 43 (1986).
[7] V. L. Kuznetsov, L. A. Kuznetsova, A. E. Kaliazin, and D. M. Rowe, J. Appl. Phys. **87**, 7871 (2000).
[8] S. Paschen, W. Carrillo-Cabrera, A. Bentien, V. H. Tran, M. Baenitz, Y. Grin, and F. Steglich, Phys. Rev. B **64**, 214404 (2001).
[9] J. D. Bryan, N. P. Blake, H. Metiu, B. B. Iversen, R. D. Poulsen, and A. Bentien, J. Appl. Phys. **92**, 7281 (2002).
[10] H. Anno, M. Hokazono, M. Kawamura, J. Nagao, and K. Matsubara, in *Proc. of 21th International Conference on Thermoelectrics* (IEEE, New York, 2002), pp. 77–80.
[11] N. P. Blake, J. D. Bryan, S. Latturner, L. Moelnitz, G. D. Stucky, and H. Metiu, J. Chem. Phys. **114**, 10063 (2001).
[12] N. P. Blake, S. Latturner, J. D. Bryan, G. D. Stucky, and H. Metiu, J. Chem. Phys. **115**, 8060 (2001).
[13] G. K. H. Madsen, K. Schwarz, P. Blaha, and D. J. Singh, Phys. Rev. B **68**, 125212 (2003).
[14] A. Bentien, M. Christensen, J. D. Bryan, A. Sanchez, S. Paschen, F. Steglich, G. D. Stucky, and B. B. Iversen, Phys. Rev. B **69**, 045107 (2004).
[15] V. Pacheco, A. Bentien, W. Carrillo-Cabrera, S. Paschen, F. Steglich, and Yu. Grin, Phys. Rev. B **71**, 165205 (2005).
[16] S. Paschen, V. Pacheco, A. Bentien, A. Sanchez, W. Carillo-Cabrera, M. Baenitz, B. B. Iversen, Y. Grin, and F. Steglich, Physica B **328**, 39 (2003).
[17] O. Maldonado, Cryogenics **32**, 908 (1992).
[18] I. Mannari, Prog. Theor. Phys. **22**, 335 (1959).
[19] J. L. Cohn, G. S. Nolas, V. Fessatidis, T. H. Metcalf, and G. A. Slack, Phys. Rev. Lett. **82**, 779 (1999).
[20] B. C. Sales, B. C. Chakoumakos, R. Jin, J. R. Thompson, and D. Mandrus, Phys. Rev. B **63**, 245113 (2001).
[21] N. F. Mott, *Conduction in Non-Crystalline Materials*, 2nd ed. (Clarendon Press, Oxford, 1993).
[22] H. Y. Fan, Solid State Phys. **1**, 283 (1955).
[23] J. M. Ziman, *Electrons and Phonons* (Oxford University Press, 1960).
[24] D. J. Kim, Prog. Theor. Phys. **31**, 921 (1964).
[25] W. R. Thurber, R. L. Mattis, Y. M. Liu, and J. J. Filliben, J. Electrochem. Soc. **127**, 1807 (1980).
[26] C. Uher, J. Yang, and S. Hu, Mater. Res. Soc. Symp. Proc. **545**, 247 (1999).
[27] G. S. Nolas, T. J. R. Weakley, J. L. Cohn, and R. Sharma, Phys. Rev. B **61**, 3845 (2000).
[28] V. Keppens, B. C. Sales, D. Mandrus, B. C. Chakoumakos, and C. Laermans, Philos. Mag. Lett. **80**, 807 (2000).
[29] B. C. Chakoumakos, B. C. Sales, and D. G. Mandrus, J. Alloys Compd. **322**, 127 (2001).
[30] A. Bentien, B. B. Iversen, J. D. Bryan, G. D. Stucky, A. E. C. Palmqvist, A. J. Schultz, and R. W. Henning, J. Appl. Phys. **91**, 5694 (2002).
[31] B. B. Iversen, A. Bentien, A. E. C. Palmqvist, J. D. Bryan, and G. D. Stucky, in *Proc. of 19th International Conference on Thermoelectrics*, edited by D. M. Rowe (BABROW Press, Wales, UK, 2000), pp. 113–116.
[32] V. Keppens, M. A. McGuire, A. Teklu, C. Laermans, B. C. Sales, D. Mandrus, and B. C. Chakoumakos, Physica B **316-317**, 95 (2002).
[33] C. Laermans, M. A. Parshin, D. A. Parshin, and V. Keppens, Physica B **316-317**, 273 (2002).
[34] I. Zerec, V. Keppens, M. A. McGuire, D. Mandrus, B. C. Sales, and P. Thalmeier, Phys. Rev. Lett. **92**, 185502 (2004).
[35] F. Bridges and L. Downward, Phys. Rev. B **70**, 140201 (2004).
[36] K. C. Sood and G. S. Verma, Phys. Rev. B **5**, 3165 (1972).
[37] J. M. Ziman, Philos. Mag. **1**, 191 (1956); *ibid.* **2**, 292(E) (1956).
[38] A. B. Pippard, Philos. Mag. **46**, 1104 (1955).
[39] A. Sergeev and V. Mitin, Europhys. Lett. **51**, 641 (2000).
[40] J. Callaway, Phys. Rev. **113**, 1046 (1959).
[41] J. E. Graebner, B. Golding, and L. C. Allen, Phys. Rev. B **34**,

5696 (1986).
[42] R. O. Pohl, Phys. Rev. Lett. **8**, 481 (1962).
[43] M. Wagner, Phys. Rev. **131**, 1443 (1963).
[44] C. R. Crosby and C. G. Grenier, Phys. Rev. B **4**, 1258 (1971).
[45] The charge carrier concentration given in Ref. 4 appears to be wrong by a factor 300, explaining the large mobility and low charge carrier mass in that report.
[46] G. A. Slack, *CRC Handbook of Thermoelectrics* (CRC Press, Boca Raton, 1995), Chap. 34.
[47] C. Wood, Rep. Prog. Phys. **51**, 459 (1988).